

AU Pegasi revisited: period evolution and orbital elements of a peculiar Type II Cepheid

Géza Csörnyei ¹ • László Szabados ²

(Submitted: 16th July; Accepted: 2nd September)

Abstract New analysis on the period changes of Type II Cepheid AU Peg is presented. The available recent photometric measurements were collected and analysed with various methods. The period has been found to be constant for certain time intervals, although increasing in overall, in contrast with the previous expectations, which suggested the period change to reverse. Superimposed on overall period change, a formerly unknown periodic behaviour has been found in the $O-C$ diagram of AU Peg, which cannot be matched to the radial velocity variations. Since the Cepheid is a member of a binary system, it is probable that the unusual period change is in connection with the companion's tidal force. The orbital elements of the binary system involving AU Peg have been also revised.

Keywords Type II Cepheids – AU Peg – period changes – binary

1 Introduction

AU Pegasi is a Type II Cepheid with a pulsation period of approximately 2.4 days and with a mean spectral type of F8. This Cepheid is considered unique in several ways; most importantly it has been found to have a

physical companion (Harris et al. (1979)) and a highly unstable pulsation period (Szabados (1977), Erleksova (1978)). The orbital period of this spectroscopic binary system is 53.3 days, which is the second shortest among the known binaries with a Type II Cepheid component. The only Type II Cepheid in a binary system with a shorter orbital period is TYC 1031 01262 1 ($P_{\text{orb}}=51.38$ days) (Antipin et al. (2007)), while the other Galactic Type II Cepheids in binary systems, IX Cas and TX Del have an orbital period of 110.29 and 130.15 days, respectively (Harris & Welch 1989).

Harris et al. (1984) found that the colour of AU Pegasi is unusually red, which would be normal for a Cepheid with a longer pulsation period. The effective temperature of its atmosphere is remarkably low, $T_{\text{eff}} = 5500 - 6000$ K, depending on the pulsational phase (Kovtyukh et al. (2018)). Recent spectroscopic measurements revealed that the $[\text{Fe}/\text{H}]$ abundance ratio is 0.27, which means that AU Peg is a metal rich Type II Cepheid (Kovtyukh et al. (2018)).

The infrared excess and the unusual colour index ($B - V=0.85$, Harris et al. (1984), Wallerstein (2002)) also indicate the presence of a dust cloud surrounding the binary system (McAlary and Welch (1986)). It has also been observed that the spectrum of this Cepheid exhibits P Cygni like behaviour, narrow emission features on the red side of the $H\alpha$ line, which show variations on orbital period timescale, thus might be a result of interaction between the atmosphere of the star with the circumstellar matter around it (Vinkó et al. (1998)). Presently it is thought that AU Pegasi is close to filling its Roche lobe and mass transfer between the two stars almost certainly occurred formerly (Maas et al. (2007)).

The temporal behaviour of the pulsation period of AU Pegasi was extensively studied by Vinkó et al. (1993) in the time interval of JD 2 433 100–2 448 600. They found that the pulsation period was slightly in-

Géza Csörnyei

László Szabados

Konkoly Observatory, Research Centre for Astronomy and Earth Sciences, Hungarian Academy of Sciences, Konkoly Thege Miklós út 15-17,

1121 Budapest, Hungary

e-mail: csornyei.geza@csfk.mta.hu

¹

Institute of Physics, Eötvös Loránd University, Pázmány Péter sétány 1/a, Budapest 1117, Hungary

²

MTA CSFK Lendület Near-Field Cosmology Research Group

creasing with a rate of $dP/dt = 5 \cdot 10^{-7}$ day/day before JD 2 440 000, while the average pulsation period length was $P_{\text{pul}} = 2.39$ days. According to their study the first epoch where the rate of the period variation changed was between JD 2 439 000 and 2 441 000. At this epoch the rate of the variation accelerated to $dP/dt = 1.8 \cdot 10^{-6}$ day/day. This period variation has eventually seemed to stop between JD 2 446 700 and 2 447 800. After this second break point the period variation seemed to reverse and to start decreasing.

They concluded that the rapid period change might be the result of the interaction between the variable star and its companion, but as they pointed out, the period variation cannot be explained by tidal interaction alone. Since the classification of Type II Cepheid is somewhat uncertain, it also had been suggested, that this variable star is a classical Cepheid crossing the instability strip for the first time (Vinkó et al. (1993)). This could explain the rapid period variation, but the latest studies still classified this variable as a Type II Cepheid (Groenewegen (2018)), which classification is also supported by the kinematics, the position of the star on the colour-magnitude diagram and length of the orbital period, as well.

The latest Gaia parallax of the object is $\Pi = 1.6739 \pm 0.0448$ milliarcsecond (Gaia Collaboration, Prusti et al. (2016), Gaia Collaboration, Brown et al. (2018)), while the V-band extinction of the star is $A_V = 0.184$ mag (NASA/IPAC Infrared Science Archive), which together correspond to an absolute magnitude of $M_V = 0.069$ mag. According to the classical Cepheid period-luminosity relation (Benedict et al. (2007)) this would correspond to a period of 0.214 days, which is significantly smaller than the one we observed, thus it supports the classification of the star as a Type II Cepheid.

In view of its importance and peculiarities, we extended the former studies with more recent photometric data covering the last 25 years. Our aim was to gain a better insight into the effect of orbital revolution on the pulsation period.

2 Observational data

In order to determine the temporal variation of the pulsation period, photometric data that have been acquired after the last extensive study (Vinkó et al. (1993)) were collected and analysed. The complete dataset contains measurements from All Sky Automated Survey (ASAS, Pojmanski (2002)), All Sky Automated Survey for Supernovae (ASAS-SN, Shappee et al. (2014)), Kamogata Sky Survey (KWS, Morokuma et al. (2014)), *Hipparcos* (Perryman et al.

Source	HJD interval	N
ASAS	2 452 754 - 2 455 157	364
ASAS-SN	2 456 389 - 2 458 380	1074
<i>Hipparcos</i>	2 447 889 - 2 448 973	75
KWS	2 455 752 - 2 458 360	509
<i>Gaia</i>	2 457 164 - 2 457 390	14

Table 1 Temporal information of the various surveys used for the analysis.

JD-2 400 000	V	$B - V$	JD-2 400 000	V	$B - V$
49538.451	9.260	1.060	51757.390	9.350	0.960
49569.531	9.240	0.910	51758.373	9.080	0.840
49570.415	9.370	0.930	51759.368	9.170	1.150
49606.326	9.390	0.910	51782.343	9.080	0.820
49606.397	9.380	0.900	51838.266	9.120	0.900
49630.240	9.390	0.950	51839.245	9.400	1.080
49630.332	9.370	0.980	51840.265	9.070	0.820
49631.235	9.080	0.750	51878.264	9.280	0.900
49631.299	9.070	0.760	52147.372	9.270	0.960
49666.208	9.270	0.920	52150.512	9.350	0.940
49666.259	9.290	0.990	52151.335	9.070	0.850
49688.211	9.360	1.010	52194.372	9.110	0.810
49690.200	9.210	0.950	52195.299	9.170	0.970
49900.448	9.330	1.000	52196.292	9.360	0.930
49918.413	9.080	0.790	52197.283	9.090	0.850
49919.431	9.330	0.920	52198.295	9.350	0.980
49920.425	9.230	0.760	52199.336	9.050	0.810
49921.428	9.150	0.960	52200.265	9.200	0.950
49952.412	9.120	0.820	52589.239	9.380	0.960
49986.433	9.060	0.930	52618.265	9.390	0.920
49987.313	9.350	0.990	52619.199	9.070	0.850
49992.273	9.430	0.930	52620.209	9.220	0.920
50015.263	9.070	0.880	52901.384	9.070	0.860
50016.285	9.400	0.970	52902.330	9.300	0.980
50018.263	9.270	0.980	52903.349	9.130	0.850
50338.429	9.100	0.950	52904.313	9.160	0.950
50371.274	9.220	0.830	52905.395	9.350	0.950
50376.366	9.090	0.780	52906.316	9.080	0.860
50605.476	9.100	0.820	52947.226	9.050	0.840
50633.482	9.320	1.000	52947.303	9.060	0.860
50634.425	9.130	0.770	52948.225	9.300	0.980
50749.268	9.330	0.990	52948.304	9.350	1.000
50749.333	9.400	0.920	53266.337	9.290	0.980
50750.274	9.110	0.790	53267.328	9.130	0.850
50750.333	9.110	0.780	53286.317	9.290	0.910
50751.246	9.150	0.960	53331.235	9.270	0.990
50751.308	9.180	0.910	53569.430	9.100	0.890
51051.396	9.190	0.820	53612.350	9.070	0.800
51052.363	9.140	0.920	53614.347	9.280	0.890
51080.300	9.200	0.810	54389.298	9.110	0.830
51756.463	9.180	0.920	54390.270	9.270	0.970

Table 2 BV photometric data obtained with the 50 cm Cassegrain telescope at Pizskéstető Mountain Station of the Konkoly Observatory.

(1997)) and *Gaia* (Gaia Collaboration, Prusti et al. (2016), Gaia Collaboration, Brown et al. (2018)).

Table 1 contains information about the temporal coverage of the photometric surveys and number of observations analysed in this paper. In addition, BV

photometric measurements obtained with the 50 cm Cassegrain telescope of the Piskésetető Mountain Station of the Konkoly Observatory by one of us (L. Sz.) between 1994 and 2007 were also involved in our study. Between 1994 and 1998, an integrating photoelectric photometer equipped with an unrefrigerated EMI 9058QB photomultiplier tube was attached to the telescope, while from the year 2000 on an electrically cooled (to -20°C) photon counting photometer containing an EMI 9203QB photomultiplier was mounted in the Cassegrain focus.

Both photometers were equipped with standard filters of the Johnson photometric system. The brightness of AU Peg was observed using BD $+17^{\circ} 4575$ as the comparison star (SIMBAD magnitudes: $V = 9.24$ mag; $B - V = 1.13$ mag), and BD $+18^{\circ} 4788$ served as the check star. Table 2 contains these previously unpublished measurements obtained in the Piskésetető Mountain Station.

Radial velocity (RV) measurement data have also been collected from the literature. In addition to the measurements made by Harris et al. (1984), three additional sets of RV data have been available: those obtained by Barnes et al. (1988), Gorynya et al. (1998) and Vinkó et al. (1998).

3 Analysis of the photometric data

Three different approaches have been used to obtain the period length of the pulsation for different time intervals: the discrete Fourier transformation (DFT, Deeming (1975)), for which we have used the Period04 analysis software (Lenz and Breger (2005)), the phase dispersion minimization (PDM, Stellingwerf (1978)) and the method of $O - C$ diagrams (Sterken (2005)). Since the first two methods require a constant or slowly varying pulsation period and for the construction of the $O - C$ diagram we would need the correct determination of the phase, e.g. the moments of a chosen phase (O) and the elapsed number of cycles (E), which would become uncertain in the case of strong period variation, the collected data had to be divided into shorter time intervals. The demonstration of this problem can be seen in Fig. 1, where the Fourier amplitude diagrams of the entire ASAS data set of AU Peg is presented. The highest peak on the upper panel corresponds to the pulsation period of $P_{\text{pul}} = 2.4122$ days. The lower panel is obtained from the residuals after the fitting of the first frequency. The highest peak in this diagram corresponds to $P = 2.4147$ days. From the proximity of these period values we assumed that the Cepheid underwent a rapid period variation in the time interval covered by the ASAS observations.

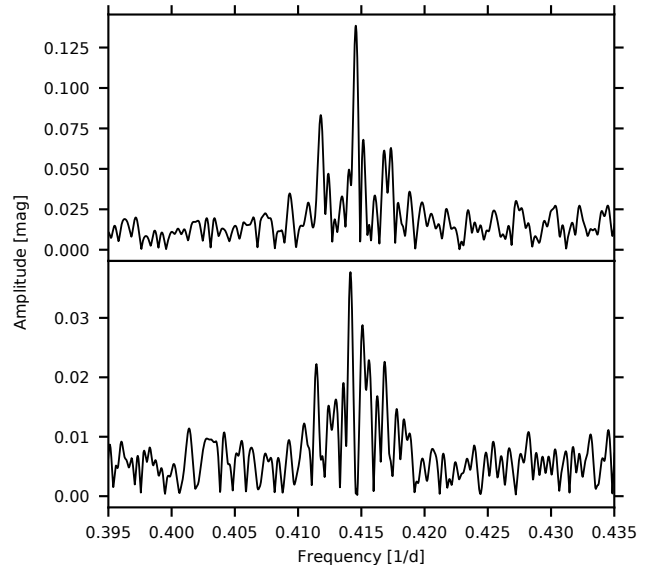


Fig. 1 The Fourier spectrum of the original ASAS data (top panel) and that of the residual data, after subtracting the main frequency (bottom panel).

Since the period variation covered by the collected data was not strong enough for the phase shift affecting the moments of light curve extrema to accumulate into a longer time than the period itself, we decided to create the $O - C$ diagram for these measurements. As a first step of the analysis, every set of observation has been split into smaller subsets. For each survey, 250 day long temporal bins were defined, in which each datapoint was moved to a new subset. The phase curves of each previously created subset of measurements have been calculated, which then were used to determine the observed (O) epoch values. This method inevitably decreases the resolution of the resulting $O - C$ curve, but the precision of the results increases, since the error of the phase calculation will decrease significantly. The $O - C$ diagram of V band measurements was calculated assuming the elements:

$$C = \text{JD } 2453481.812 + 2.412^{\text{d}} \cdot E.$$

The obtained $O - C$ values are listed in Table 4, while the corresponding diagram is presented in Fig. 2.

It has been found that the segments of the $O - C$ graph can be described with linear functions, thus the pulsation period of the Cepheid remains approximately the same for the different time intervals. The change of the pulsation period shown by the ASAS data can be approximated as a parabolic function on the $O - C$ diagram, hence it can be described as a linear period change (see later in this chapter). Table 3 describes

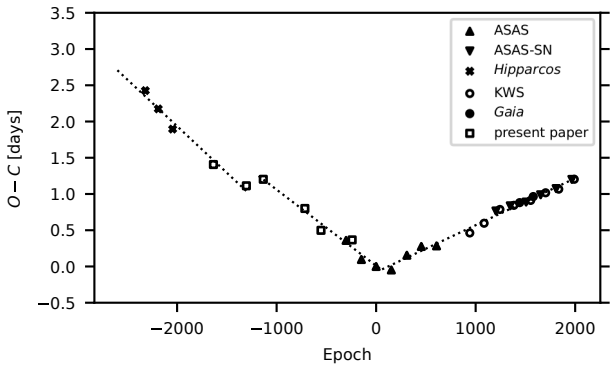


Fig. 2 The $O - C$ diagram of AU Pegasi calculated from the new measurements with linear fit segments.

the linear fits in the different time intervals. As illustrated in Fig. 3, it has been found that the $O - C$ data points obtained from ASAS, ASAS-SN and KWS measurements deviate from the fitted linear curve in a periodic manner.

Epoch	Linear fit	Period [d]
$-2600 < E < -1280$	$-0.0013 \cdot E - 0.0636$	2.4109
	$\pm 0.00013 \quad \pm 0.0851$	± 0.0001
$-1180 < E < 60$	$-0.0010 \cdot E + 0.0108$	2.4111
	$\pm 0.00014 \quad \pm 0.0562$	± 0.0001
$60 < E < 2000$	$0.0006 \cdot E - 0.0780$	2.4128
	$\pm 0.00002 \quad \pm 0.0243$	± 0.0001

Table 3 The fitted lines for the different time intervals (see Fig. 2), and the calculated periods.

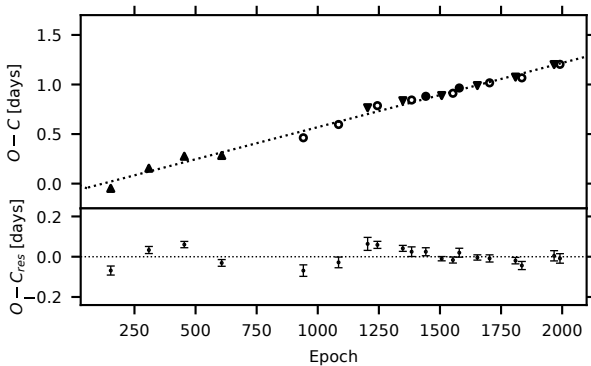


Fig. 3 Top panel: The last linear segment of the $O - C$ diagram and its linear fit. Bottom panel: The residual values of the $O - C$ diagram after subtracting the linear fit. The notation of the data points is the same as in Fig. 2.

The period of this cyclic behaviour is approximately 2215 days, while its amplitude is 0.05 days. This variation cannot originate from the light-time effect caused

by the known companion of the Cepheid, since the expected amplitude of this variation would be as low as 0.001 days, and the period is not appropriate, either. To examine whether the obtained periodic variation could correspond to the light-time effect of a formerly unknown companion, we analysed the available RV observations collected from the literature. The Fourier spectra of the RV observations before and after subtracting the main frequency (the known orbital motion) are presented in Fig. 4. Since the expected RV projection corresponding to the obtained period and amplitude of the variation is 45.7 km/s (assuming circular orbit), which would then result in a sharp peak in the Fourier diagram of the RV observations at the frequency of $4.515 \cdot 10^{-4}$ cycles/day, that is clearly not present (although the Fourier spectrum shows a peak with a much smaller amplitude at that frequency), we cannot attribute the observed variation to any effect caused by the orbital motion of the Cepheid.

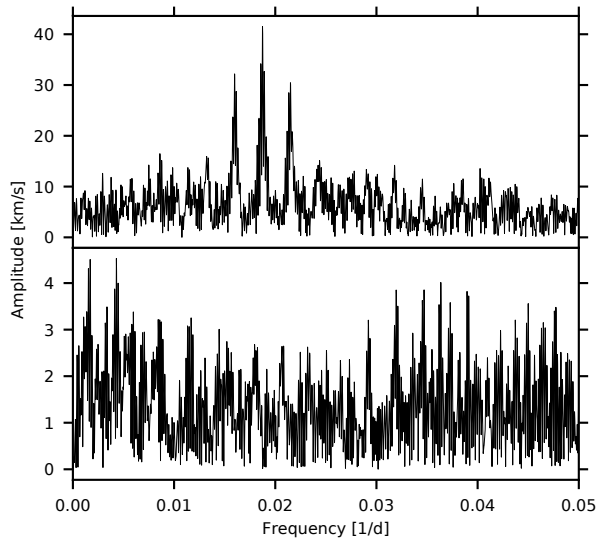


Fig. 4 The Fourier spectrum obtained from the RV measurements (top panel) and that of the residual data after whitening with the frequency of the known orbital motion.

In the case of most archival photometric data series and the measurements presented in this paper as well, not only V band, but B band observations were also available. With the use of available B band data, another set of O values has been calculated. Since these measurements covered the time interval in which a rapid period increase was observed (Vinkó et al. (1993)), the $O - C$ diagram of B band could not have been created, but the simultaneous V and B observations allowed the comparison of B and V band epochs. The differences of the same phase O values calculated from B and V band observations are presented in Fig. 5.

HJD-2 400 000	E	$O - C$ (d)	σ (d)	Survey
47888.061	-2319	2.427	0.016	<i>Hipparcos</i>
48201.388	-2189	2.174	0.020	<i>Hipparcos</i>
48548.458	-2045	1.895	0.019	<i>Hipparcos</i>
49536.949	-1635	1.407	0.031	present paper
49898.720	-1485	1.356	0.032	present paper
51755.516	-716	0.800	0.060	present paper
52145.983	-554	0.499	0.039	present paper
52753.705	-302	0.360	0.021	ASAS
52900.852	-241	0.367	0.043	present paper
53124.911	-148	0.096	0.026	ASAS
53481.812	0	0.000	0.014	ASAS
53850.823	153	-0.048	0.022	ASAS
54227.321	309	0.155	0.018	ASAS
54577.203	454	0.276	0.015	ASAS
54946.269	607	0.284	0.016	ASAS
55752.104	941	0.462	0.028	KWS
56099.587	1085	0.597	0.026	KWS
56386.801	1204	0.766	0.032	ASAS-SN
56483.308	1244	0.787	0.018	KWS
56734.221	1348	0.837	0.015	ASAS-SN
56821.065	1384	0.843	0.024	KWS
56961.008	1442	0.881	0.019	<i>Gaia</i>
57117.804	1507	0.888	0.011	ASAS-SN
57228.786	1553	0.912	0.015	KWS
57291.555	1579	0.965	0.020	<i>Gaia</i>
57470.078	1653	0.989	0.013	ASAS-SN
57590.713	1703	1.067	0.018	KWS
57846.458	1809	1.074	0.025	ASAS-SN
57909.167	1835	1.067	0.020	KWS
58227.704	1967	1.201	0.024	ASAS-SN
58285.598	1991	1.203	0.024	KWS

Table 4 $O - C$ values of AU Peg calculated from the seasonal V band datasets of the different surveys.

Table 5 contains the calculated differences of the two sets of O values. According to the results, the brightness maximum in the B band light curve precedes the V band with approximately 0.082 days ($\Delta\phi = 0.039$ for the phase shift). This corresponds well to the former observations (Freedman 1988), where a systematic phase shift was found for several Cepheids, which appeared to be increasing for longer wavelengths. All photometric measurements have also been analysed with the DFT and PDM methods. To prevent the mixing of different period values, observation subsets shorter than 250 days were created. Data from different surveys were treated separately. For the PDM method parameters $N_b=10$ and $N_c=3$ have been used, where N_b and N_c denote the number of bins and the number of covers (Stellingwerf (1978)).

Some of the datasets, like the ASAS-SN observations, proved to contain significant number of outliers and exhibit a higher scatter in the data, which would result in less precise period evaluation. To address this problem

during the PDM fit, the outlying data points deviating from the calculated phase curve with more than 2σ were excluded, and the phase curve was calculated again. We have tested the method with different thresholds and the 2σ cut appeared to be the best choice for an automated outlier removal: with the 1σ threshold many points were removed that could not have been flagged as definite outliers, while at 3σ not all outliers were removed. An example for the V band phase curve of the Cepheid is presented in Fig. 6.

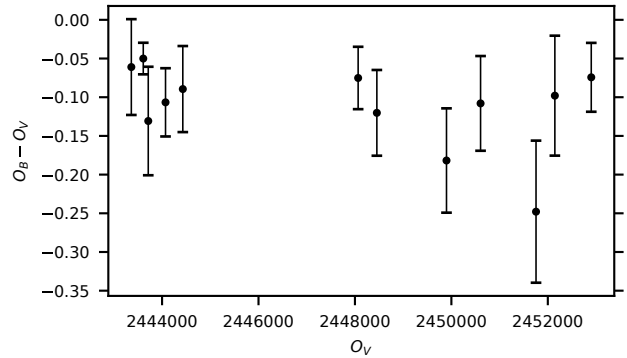


Fig. 5 The differences of the O values in B and V bands in days as a function of the Julian Day.

HJD-2 400 000	$O_B - O_V$	σ	Reference
43362.532	-0.061	0.062	Vinkó et al. (1993)
43610.115	-0.050	0.021	Henden (1980)
43713.625	-0.131	0.070	Vinkó et al. (1993)
44071.742	-0.107	0.044	Moffett (1984)
44430.211	-0.089	0.056	Moffett (1984)
48066.403	-0.075	0.041	Vinkó et al. (1993)
48454.503	-0.120	0.055	Vinkó et al. (1993)
49898.720	-0.182	0.067	present paper
50605.330	-0.108	0.061	present paper
51755.516	-0.248	0.092	present paper
52145.983	-0.098	0.078	present paper
52900.852	-0.074	0.045	present paper

Table 5 The time difference of the moments of brightness maxima and its standard deviation (σ) in different bands in days.

Table 6 contains the calculated period values for the different surveys and various methods. The period has been calculated with every method, if the temporal coverage and the amount of data points in the seasonal subset allowed it. For the ASAS, ASAS-SN and KWS the period has been calculated with every method. In the case of the *Gaia* data, the amount of measurements and the short term coverage allowed the use of DFT, while the number of data points was insufficient to calculate

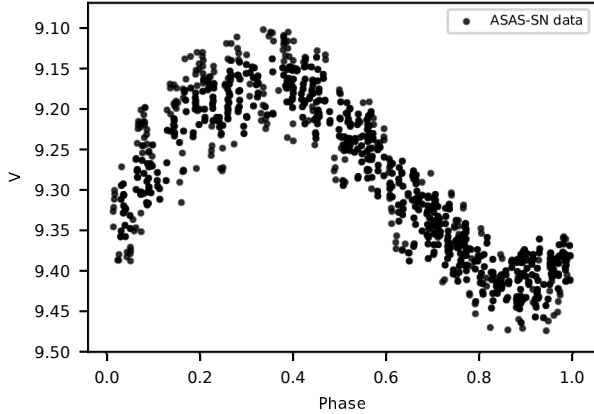


Fig. 6 Light curve in V calculated from the ASAS-SN data. The phases were calculated using the periods listed in Table 6.

the pulsation period properly with PDM. Since the time interval of the *Gaia* photometric data was covered by ASAS-SN and KWS observations, the period was calculated with the help of $O-C$ method as well. The photometric data obtained by *Hipparcos* had to be treated differently, since the measurements covered only short time, but the amount of data points was larger than in the case of *Gaia* measurements. This time interval was not covered by any other surveys, thus the pulsation period was only calculated with DFT and PDM for this survey. In the case of the data obtained at Pizskéstető Observatory, the measurements were scattered in time and covered several years. For this reason, the pulsation period was only calculated with $O-C$ method. The final period value was the average of the pulsation periods obtained with the different methods for every survey (Table 6). The pulsation period of AU Peg is presented as a function of time in Fig. 7.

According to the *Hipparcos* and Pizskéstető measurements, the pulsation period of AU Pegasi was slightly increasing between HJD 2448500 and 2452000 at a rate of $8.348 \cdot 10^{-5}$ day/year. Between HJD 2452900 and 2454850 the rate of the period change increased according to the ASAS measurements, to the value of $3.746 \cdot 10^{-4}$ day/year, which is approximately half of the rate the pulsation period had been changing with between HJD 2442500 and 2446000. After this rapid change, the period seemed to keep its value, and it remained constant until the latest observations. This behaviour has not been observed before and it is still an open question, how the companion of the Cepheid affects the pulsation, and if there is a direct connection between the evolution of the period and binarity of the star.

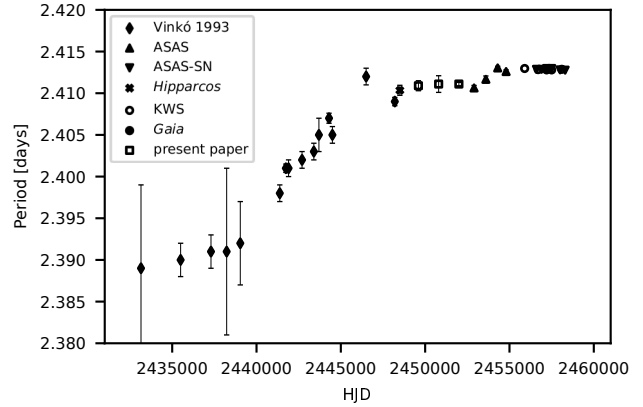


Fig. 7 The pulsation period of AU Pegasi as a function of time

4 Revised spectroscopic orbit of AU Peg

The orbital elements of the binary system involving AU Peg have been determined by Harris et al. (1984) based on their own RV data. When revising the elements of the spectroscopic orbit, the available RV data (i.e. those published by Harris et al. (1984), Barnes et al. (1988), Gorynya et al. (1998) and Vinkó et al. (1998)) were split into subsets covering no more than two years. These data sets then have been corrected for variations due to the pulsation by fitting and subtracting the sinusoidal changes corresponding to the pulsation period and its first harmonic. The amplitude ratio of the two fitted components is 10:1. The second harmonic can be neglected, since its amplitude is not large enough to make the signal distinguishable from the noise in the Fourier spectrum. Since the pulsation period of the Cepheid was changing significantly during and between the different RV measurements, we used the diagram shown in Fig. 7 to obtain the correct value for the pulsation period. While subtracting the contribution of the first harmonic from the RV data, we assumed that the RV amplitude ratio of the fundamental and first harmonic variation is the same as in the case of the light curve. To obtain the orbital parameters we fitted

$$v_i = V - K(\cos(f_i + \bar{\omega}) + e \cos \bar{\omega})$$

to the pulsation corrected dataset, where v_i denotes the i th RV entry corresponding to f_i true anomaly at time entry t_i . In the formula above, V is the systemic velocity of the system, K is the semi-amplitude of the variation, e is the eccentricity of the orbit, and $\bar{\omega}$ is the argument of the periastris (Fulton et al. 2018). To calculate the mean anomalies at various time entries we also had to

Survey	T	P_{DFT}	P_{PDM}	P_{O-C}	P_{final}
ASAS	52900	2.4103	2.4105	2.4111	2.4106
		± 0.0002	± 0.0001	± 0.0001	± 0.0003
	53600	2.4119	2.4119	2.4111	2.4117
		± 0.0001	± 0.0001	± 0.0001	± 0.0003
	54300	2.4133	2.4130	2.4128	2.4130
	± 0.0001	± 0.0002	± 0.0001	± 0.0002	
	54800	2.4124	2.4126	2.4128	2.4126
	± 0.0009	± 0.0003	± 0.0001	± 0.0004	
ASAS-SN	56600	2.4128	2.4130	2.4128	2.4129
		± 0.0007	± 0.0003	± 0.0001	± 0.0002
	56900	2.4128	2.4130	2.4128	2.4129
		± 0.0008	± 0.0002	± 0.0001	± 0.0002
	57200	2.4129	2.4132	2.4128	2.4130
		± 0.0004	± 0.0001	± 0.0001	± 0.0002
	57500	2.4127	2.4134	2.4128	2.4130
	± 0.0002	± 0.0002	± 0.0001	± 0.0002	
	58000	2.4126	2.4130	2.4128	2.4128
	± 0.0009	± 0.0002	± 0.0001	± 0.0002	
	58300	2.4127	2.4128	2.4128	2.4128
	± 0.0004	± 0.0001	± 0.0001	± 0.0001	
<i>Gaia</i>	57200	2.4128	–	2.4128	2.4128
	± 0.0003			± 0.0001	± 0.0001
<i>Hipparcos</i>	48500	2.4103	2.4104	–	2.4104
	± 0.0002	± 0.0001			± 0.0001
KWS	55900	2.4131	2.4130	2.4128	2.4130
		± 0.0002	± 0.0001	± 0.0001	± 0.0001
	56700	2.4127	2.4130	2.4128	2.4128
		± 0.0003	± 0.0001	± 0.0001	± 0.0002
	57500	2.4127	2.4129	2.4128	2.4128
	± 0.0003	± 0.0001	± 0.0001	± 0.0001	
	58100	2.4129	2.4129	2.4128	2.4129
	± 0.0002	± 0.0002	± 0.0001	± 0.0001	
Present paper	49600	2.4110	–	2.4109	2.4109
		± 0.0021		± 0.0001	± 0.0006
	50800	2.4113	–	2.4111	2.4111
		± 0.0033		± 0.0001	± 0.0010
	52000	2.4112	–	2.4111	2.4111
	± 0.0002		± 0.0001	± 0.0002	

Table 6 The pulsational period values calculated from the seasonal data of different surveys. T : HJD–2 400 000; P : the obtained period in days.

fit the periastron passage factor χ , which is the fraction of orbit prior to the start of data-taking that periastron occurred.

We used a Bayesian approach to fit the RV data and extracted the orbital parameters along with their uncertainties using Markov Chain Monte Carlo (MCMC) simulations. To implement this method we have used the `radvel` python package introduced and described in Fulton et al. (2018). The prior distributions were chosen to be uniform centered on the parameters obtained in Harris et al. (1984), except for the eccentricity and the longitude of the periastron, for which every possible value was considered. The obtained fit along with the orbital RV phase curve is presented in Fig. 8.

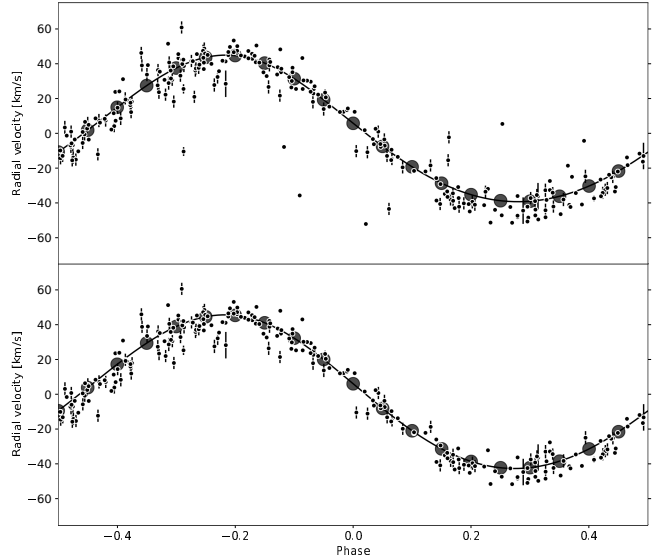


Fig. 8 The orbital RV curve (after correcting for the pulsation) and the obtained fit. Top panel: the obtained fit with the discrepant datapoints included. Bottom panel: the fit obtained after removing these points.

The computed elements are

$$P = 53.3344 \pm 0.0003 \text{ d}$$

$$V = -1.6368 \pm 0.0004 \text{ km/s}$$

$$K = 44.091 \pm 0.592 \text{ km/s}$$

$$e = 0.0425 \pm 0.0027$$

$$\chi = 0.3264 \pm 0.0005$$

$$\bar{\omega} = 0.3404 \pm 0.0040 \text{ rad.}$$

We have compared these orbital elements to those obtained in Harris et al. (1984). According to our study, the orbit is fairly different from the previously assumed one: the orbital period appears to be longer than obtained before (53.319 ± 0.015 days) and the calculated amplitude of variation is larger by 2.2 km/s than the previous one, as well. The eccentricity of the orbit appears to be smaller, thus according to our calculations, the orbit itself is more circular, than it was originally believed ($e = 0.12 \pm 0.04$, Harris et al. (1984)). It has been mentioned in Harris et al. (1984), that by omitting a discrepant point from their dataset, they obtained an orbit with smaller eccentricity, which is more similar to the solution we obtained. Since for the solution above we discarded all discrepant points (through creating the phase curve in every 250 day long time interval supposing a sinusoidal change, then removing the outliers with the help of the previously shown 2σ clipping) we tested whether the orbit obtained from the original data, including the previously deleted points, would be more similar to the one in Harris et al. (1984). In this case

the period remained the same, but the amplitude decreased by 2 km/s, thus its value became very similar to that obtained in Harris et al. (1984). The eccentricity of the orbit turned out to be larger than in the first case ($e = 0.068 \pm 0.004$) due to these discrepant datapoints. Although this value is within the error limits given in Harris et al. (1984), it still corresponds to a more circular orbit and we believe, that omitting the discrepant datapoints is a reasonable choice, considering their high scatter from the fitted phase curve (Fig. 8.).

5 Summary

It has been presented that, in contrast to the previous behaviour of AU Pegasi, the rate of pulsation period change has decreased significantly and the period has come to a constant value, according to the latest observations. The last data point from the analysis of Vinkó et al. (1993) suggests that there might have been another time interval (between JD 2445 000 and 2 447 500), when the pulsation period set in a constant value over time, followed by a rapid period change. If this behaviour turns out to be periodic, it might be an indicator for the interaction between the Cepheid and its companion.

According to our analysis, a wave in the $O - C$ diagram has been found, which could not have been connected to any known physical process in the environment of the Cepheid. The amplitude and period of this variation might correspond well to light-time effect, but the lack of this periodicity in the RV data rules this possibility out. This effect might be the result of the tidal interaction between the Cepheid and its companion, but to support this hypothesis, further observations and analysis would be required.

We have also revised the spectroscopic orbit of AU Peg. By subtracting the contributions of the pulsation from the RV data taking into account the strong changes observed in the pulsation period (see Fig. 7) and by using Bayesian framework for the fitting, we could reliably determine the orbital elements of AU Peg. According to our analysis, the orbit of AU Peg is more circular than it was previously determined, regardless how one handles the discrepant datapoints (the eccentricity obtained in the case of the whole dataset is $e = 0.068 \pm 0.004$, while after removing the mentioned datapoints the fitting process resulted in $e = 0.0425 \pm 0.0027$). The resulting amplitude of the RV variation and the orbital period values were larger than the ones obtained in Harris et al. (1984), which, together with the smaller eccentricity, indicate higher mass function for the companion star.

The peculiar behaviour of the pulsation period of AU Pegasi necessitates frequent photometric observations of this interesting binary system with a Type II Cepheid component.

Acknowledgements This project has been supported by the GINOP-2.3.2-15-2016-00003 grant of the Hungarian National Research, Development and Innovation Office (NKFIH). This work has been partly supported by the Lendület Program of the Hungarian Academy of Sciences, project No. LP2018-7/2018 and the Hungarian NKFIH projects K-115 709 and K-129 249.

References

- Antipin, S.V., Sokolovsky, K.V., Ignatieva, T.I.: *Mon. Not. R. Astron. Soc.* **379**, 60 (2007)
- Barnes, I. T. G., Moffett, T.J., Slovak, M.H.: *Astrophys. J. Suppl. Ser.* **66**, 43 (1988)
- Benedict, G.F., McArthur, B.E., Feast, M.W., Barnes, T.G., Harrison, T.E., Patterson, R.J., Menzies, J.W., Bean, J.L., Freedman, W.L.: *Astron. J.* **133**, 1810 (2007)
- Deeming, T.J.: *Astrophys. Space Sci.* **36**(1), 137 (1975)
- Erleksova, G.E.: *Peremennye Zvezdy* **21**, 97 (1978)
- Fulton, B.J., Petigura, E.A., Blunt, S., Sinukoff, E.: *Publ. Astron. Soc. Pac.* **130**, 044504 (2018)
- Gaia Collaboration, Brown, A.G.A., Vallenari, A., Prusti, T., de Bruijne, J.H.J., Babusiaux, C., Bailer-Jones, C.A.L., Biermann, M., Evans, D.W., Eyer, L., *et al.*: *Astron. Astrophys.* **616**, 1 (2018)
- Gaia Collaboration, Prusti, T., de Bruijne, J.H.J., Brown, A.G.A., Vallenari, A., Babusiaux, C., Bailer-Jones, C.A.L., Bastian, U., Biermann, M., Evans, D.W., *et al.*: *Astron. Astrophys.* **595**, 1 (2016)
- Gorynya, N.A., Samus', N.N., Sachkov, M.E., Rastorguev, A.S., Glushkova, E.V., Antipin, S.V.: *Astronomy Letters* **24**, 815 (1998)
- Groenewegen, M.A.T.: *Astron. Astrophys.* **619**, 8 (2018)
- Harris, H., Olszewski, E.W., Wallerstein, G.: *Astron. J.* **84**, 1598 (1979)
- Harris, H.C., Olszewski, E.W., Wallerstein, G.: *Astron. J.* **89**, 119 (1984)
- Kovtyukh, V., Yegorova, I., Andrievsky, S., Korotin, S., Saviane, I., Lemasle, B., Chekhonadskikh, F., Belik, S.: *Mon. Not. R. Astron. Soc.* **477**, 2276 (2018)
- Lenz, P., Breger, M.: *Communications in Asteroseismology* **146**, 53 (2005)
- Maas, T., Giridhar, S., Lambert, D.L.: *Astrophys. J.* **666**, 378 (2007)
- McAlary, C.W., Welch, D.L.: *Astron. J.* **91**, 1209 (1986)
- Morokuma, T., Tominaga, N., Tanaka, M., Mori, K., Matsumoto, E., Kikuchi, Y., Shibata, T., Sako, S., Aoki, T., Doi, M., *et al.*: *Publ. Astron. Soc. Japan* **66**(6), 114 (2014)
- Perryman, M.A.C., *et al.*: *Astron. Astrophys.* **323**, 49 (1997)
- Pojmanski, G.: *Acta Astron.* **52**, 397 (2002)
- Shapsee, B., *et al.*: In: *American Astronomical Society Meeting Abstracts #223*. American Astronomical Society Meeting Abstracts, vol. 223, p. 236 (2014)
- Stellingwerf, R.F.: *Astrophys. J.* **224**, 953 (1978)
- Sterken, C.: In: Sterken, C. (ed.) *The Light-Time Effect in Astrophysics: Causes and cures of the O-C diagram*. ASP Conf. Ser., vol. 335, p. 3 (2005)
- Szabados, L.: *Communications of the Konkoly Observatory, Hungary* **70**, 1 (1977)
- Vinkó, J., Szabados, L., Szatmáry, K.: *Astron. Astrophys.* **279**, 410 (1993)
- Vinkó, J., Evans, N.R., Kiss, L.L., Szabados, L.: *Mon. Not. R. Astron. Soc.* **296**, 824 (1998)
- Wallerstein, G.: *Publ. Astron. Soc. Pac.* **114**, 689 (2002)